




Instantaneous measurement of high-power millimeter-wave beam for 28 GHz gyrotron

Cite as: Rev. Sci. Instrum. **90**, 024703 (2019); <https://doi.org/10.1063/1.5050957>

Submitted: 04 August 2018 . Accepted: 19 January 2019 . Published Online: 05 February 2019

Maho Matsukura, Kohei Shimamura , Masatoshi Suzuki, Mizojiri , Shigeru Yokota, Ryutaro Minami, Tsuyoshi Kariya , and Tsuyoshi Imai



View Online



Export Citation



CrossMark

ARTICLES YOU MAY BE INTERESTED IN

[An adaptive calibration technique of timing skew mismatch in time-interleaved analog-to-digital converters](#)

Review of Scientific Instruments **90**, 025102 (2019); <https://doi.org/10.1063/1.5063660>

[An x-band continuous wave saturation recovery electron paramagnetic resonance spectrometer based on an arbitrary waveform generator](#)

Review of Scientific Instruments **90**, 024102 (2019); <https://doi.org/10.1063/1.5043316>

[The spectral background problem of portable fiber Raman instruments and a solution for the on-site detection of extremely weak signals](#)

Review of Scientific Instruments **90**, 023101 (2019); <https://doi.org/10.1063/1.5064398>



JANIS

Janis Dilution Refrigerators & Helium-3 Cryostats
for Sub-Kelvin SPM

Click here for more info www.janis.com/UHV-ULT-SPM.aspx



Instantaneous measurement of high-power millimeter-wave beam for 28 GHz gyrotron

Cite as: *Rev. Sci. Instrum.* **90**, 024703 (2019); doi: [10.1063/1.5050957](https://doi.org/10.1063/1.5050957)

Submitted: 4 August 2018 • Accepted: 19 January 2019 •

Published Online: 5 February 2019



Maho Matsukura,¹ Kohei Shimamura,^{1,a)}  Masatoshi Suzuki,¹ Mizojiri,¹  Shigeru Yokota,¹ Ryutaro Minami,² Tsuyoshi Kariya,²  and Tsuyoshi Imai²

AFFILIATIONS

¹Department of Energy and Mechanical Engineering, University of Tsukuba, Tsukuba, Japan

²Plasma Research Center, University of Tsukuba, Tsukuba, Japan

^{a)}Email: shimamura@kz.tsukuba.ac.jp

ABSTRACT

An instantaneous measurement system of high-power millimeter-wave was proposed and demonstrated with a 28 GHz gyrotron at the Plasma Research Center, University of Tsukuba. The high-power detector consists of an attenuator and a linear polarized microstrip antenna with an F-class load rectifier, which is a commonly used system for radio-frequency wireless power transmission. The detector obtained the power distribution of the gyrotron output beam which showed good agreement with the infrared camera image. The rectenna array detector received 45 W RF input power with a 0.4 ms response time. The results revealed that the proposed narrow band detector is useful as an imaging sensor and power meter for high-power millimeter-wave beam output with a wide wavelength range.

Published under license by AIP Publishing. <https://doi.org/10.1063/1.5050957>

I. INTRODUCTION

Millimeter wave detection has been attractive for use in scientific measurements for high-temperature gas and foreign matter inspection at airport security gates and factories because the object transmittance of the millimeter wave is better than that of visible or infrared (IR) light sources or terahertz waves.¹ For imaging applications, the millimeter wave spatial resolution is better than that of the microwave or UHF bands. Millimeter wave imaging is widely used for scientific measurements in fields such as astrophysics, nuclear fusion physics, and combustion research. In plasma fusion research, plasma diagnostics and the characterization of millimeter wave beams are the main topics of millimeter wave detection.^{2,3} Recently, the beam transmission of high-power millimeter waves has become attractive for the atmospheric discharge phenomena of millimeter wave, and the wireless power transmission for the mobile application.⁴⁻⁸ For such applications, a gyrotron is useful as a high-power millimeter-wave beam source with maximum output power and frequency, respectively, of 1.5 MW and 1 THz.⁹

There are three strategies to obtain the gyrotron beam profile, such as the calorimetric method, the IR visualization, and the diode method. The calorimetric method requires a water chamber with a thermistor sensor or a thermoelectric transducer.^{10,11} An infrared camera is available for power distribution measurements. However, the local RF power intensity is unknown.¹² The spatial and temporal resolution of the infrared camera and the water load measurement are regulated by the thermal properties of the material. These conventional detection devices are difficult to use in situations that require high-power and high-speed millimeter wave radiation. The idea of the present paper is similar to the third strategy. Several previous studies were conducted to obtain the two-dimensional intensity distribution of the millimeter-wave beam using the diode. Chirkov presented two methods for millimeter wave phase front reconstruction of paraxial linear polarized wave beams at the mW power level and the frequency 140 GHz.¹³ Kasperek and Hornstein recorded the beam patterns by using a small waveguide probe (or like waveguide) and an x-y scanner.^{14,15} Recently, semiconductor-based commercial products offering millimeter and terahertz

imaging have become available, but their detection power is simply low-level RF input.¹⁶

This paper describes our proposed high-power and high-speed millimeter wave detection using a rectenna consisting of the rectifier and antenna. The rectenna is widely used for RF energy harvesting and wireless power transfer. Therefore, the rectenna benefits are its wide operation frequency (RF-0.3 THz)⁸ and its instantaneous measurement of the gyrotron output beam. The rectenna circuit design, which consists of the antenna, diode, and filter, is quite simple and inexpensive compared to a conventional heterodyne system. Furthermore, the natural frequency of a rectenna, determined by the rise time of the diode, is higher than 10 MHz. For this study, a 28 GHz Ka-band rectenna was developed and demonstrated as a high-speed camera element using a 28 GHz 0.5 MW gyrotron at the Plasma Research Center, University of Tsukuba, Japan.¹⁷ The frequency of 28 GHz has attracted attention in various applications, such as material processing, the plasma heating, and the next mobile communication (5G). A gyrotron at 28 GHz has been successfully developed as a product at CPI (200 kW/CW) and IAP/GYCOM (28 GHz/15 kW/pulse or CW and 28 GHz/400 kW/0.1 s).¹⁸⁻²¹ We demonstrated the rectenna detector as a camera and a power meter. First, the power distribution of the beam profile for gyrotron was obtained and compared with the infrared camera. Finally, the rectenna array was developed and demonstrated as a power meter for the gyrotron.

II. DESIGN AND CHARACTERISTICS OF DETECTOR ELEMENTS

A. Design of camera elements

Figure 1 shows the rectenna, which consists of a microstrip antenna array (a) and a rectifying circuit (c). A cross-section of the rectenna is also shown (e). Single elements of the rectenna were 24 mm × 22.5 mm. The upper side is the antenna array. The lower side is the rectifier circuit. The four elements of the microstrip square patch antenna were combined to the feeding point. The rectifying circuit is a single shunt rectifier with a Class-F load, as proposed in Ref. 22. The fundamental frequency, the second frequency and third harmonics frequency do not pass through the Class-F load circuits. The designed antenna array and the rectifying circuit are bonded together, ground plane to ground plane, with a conductive paste and are interconnected via a 0.2 mm diameter copper wire. The rectifier has a diode (MA4E1317; Macom). The microstrip line width is 0.4 mm. DiClad880 (Rogers Corp.) ($\epsilon_r = 2.17$, $\tan \delta = 0.0008$) was used as a dielectric substance with a circuit board plotter (Eleven Lab; MITS Electronics).

Antenna parameters such as the S_{11} parameter and the radiation pattern in the H-plane were simulated, respectively, using a commercial simulator (EMPro; Keysight Technologies, Inc.) and were measured using a scalar network analyzer system (83620A, 8757D, 83554A; Keysight Technologies, Inc.). The measured and simulated S_{11} parameters at 28 GHz were respectively -12.9 dB and -32.26 dB. The results indicated the reflection of the antenna as less than 10% at the operating

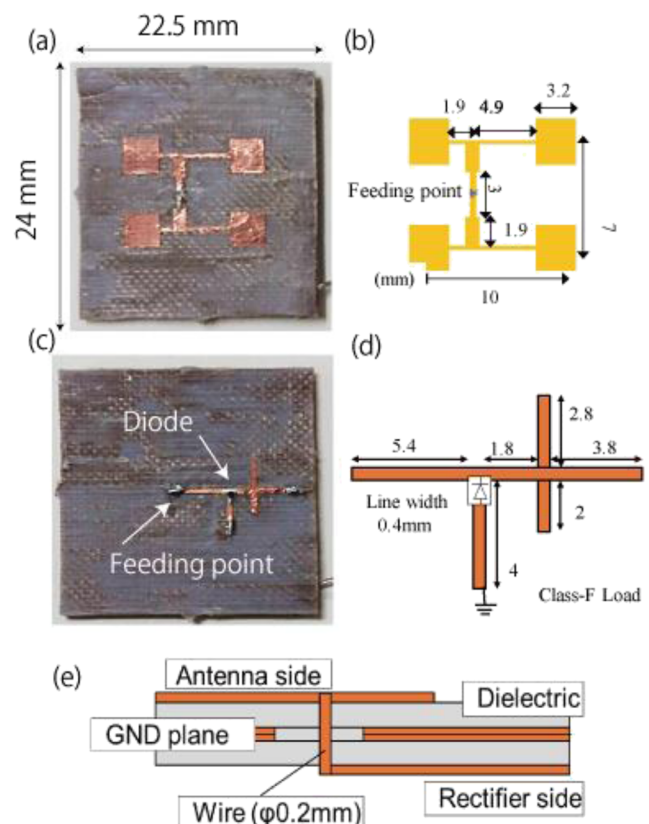


FIG. 1. Schematic of the rectenna: microstrip antenna array (a) and (b), rectifying circuit (c) and (d), and rectenna cross-section (e). All dimensions are in millimeters.

frequency. S_{11} has a large difference in measurement and simulation. However, the calibration of the circuit including this reflection value is performed, so there is no problem with the RF-beam measurement. Figure 2 shows the measured and simulated radiation patterns. The antenna gain was measured as 9.0 dBi at 28 GHz.

Figure 3 portrays the RF-DC conversion efficiency and its output power as a function of input power. A Gunn oscillator (QBY-2830CJ, QuinStar Tech., Inc.) with an isolator (QuinStar, QIF-A00000), a variable attenuator (WAT-345, Nihon

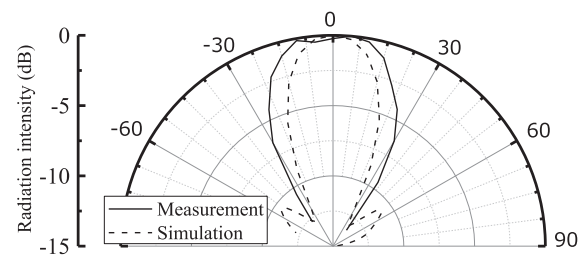


FIG. 2. Simulated and measured radiation patterns of the designed array antenna at 28 GHz.

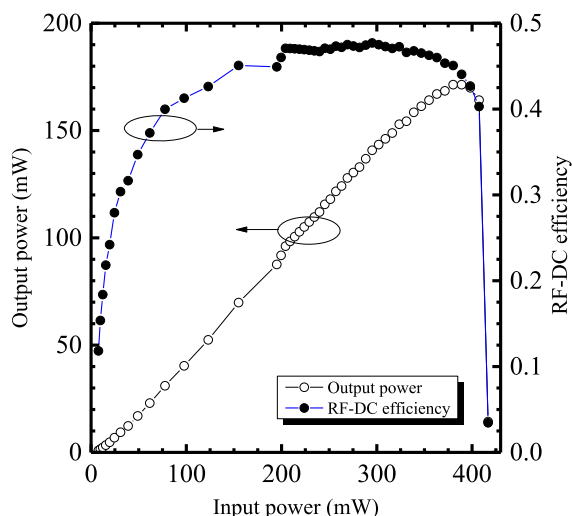


FIG. 3. RF-DC conversion efficiency and output power with 130 Ω DC load at 28 GHz.

Koshuha, Co., Inc.), and a 10 dB directional coupler (WDK-347D, Nihon Koshuha Co., Ltd.) with the power meter and a mode converter from WR-28 waveguide to K-type coaxial cable were used to obtain the RF-DC conversion efficiency. The maximum RF-DC efficiency at 130 Ω DC load was 47.7%. The output power was 140.8 mW at 295.1 mW input power. The breakdown threshold of the rectifier was 410 mW input power. The measured RF-DC conversion efficiency

was found to be comparable to those reported from other studies.^{23,24}

III. POWER DISTRIBUTION MEASUREMENT USING 400 kW CLASS GYROTRON

A. Experimental setup: Gyrotron and test chamber

The 28 GHz 0.5 MW gyrotron at the Plasma Research Center, University of Tsukuba, was used to demonstrate the millimeter wave detector. Figure 4 portrays a schematic diagram of the gyrotron experiment (a) and the setup in the test chamber (b). The high-power millimeter wave beam was introduced to a shielded room (2 × 2 × 2 m) from the gyrotron aperture window by the 63.5-mm-diameter corrugated waveguide. The RF test chamber (1 × 1 × 1.5 m) was set in the shield room. Microwave absorbers were used in the RF test chamber to avoid RF wave reflection and interference. The distance between the millimeter wave detector and the corrugated waveguide aperture was 0.9 m. Figure 4(c) portrays the transmission line between the gyrotron and the chamber. At the first miter bend, the RF monitor was installed and its signal was shown in Fig. 7. To monitor the gyrotron output signal, the array detectors were developed as a “power meter.” Figures 4(d)–4(f) show the rectenna array and its circuit pattern. The rectenna array consists of 25 elements with a size of 120 mm × 112.5 mm. As presented in Fig. 4(f), five rectenna elements were connected in parallel. The five rectenna array was connected in series.

Table I portrays the gyrotron operation condition. The gyrotron output power was set at 52.9 kW with 2 ms pulse

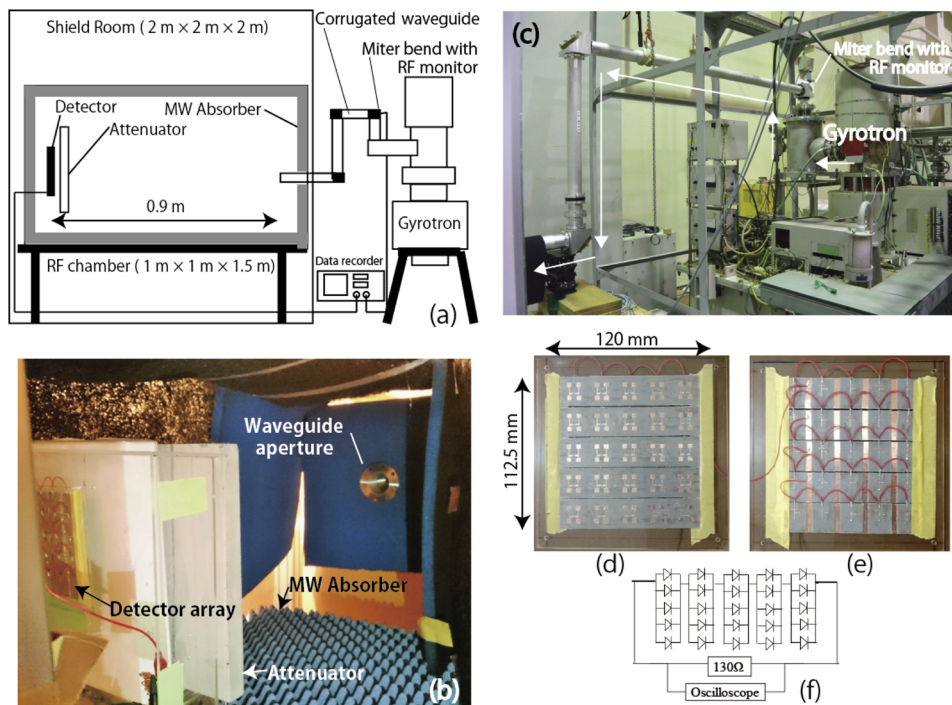


FIG. 4. Schematic of the gyrotron experiment (a), setup in the test chamber (b), the transmission line from the gyrotron to the chamber(c), and rectenna array 5 × 5 elements: antenna side (d), rectifier side (e), and the circuit pattern of the array (f).

TABLE I. Gyrotron operation conditions.

| | |
|---------------------|-----------------------------------|
| Frequency (GHz) | 28 |
| Output power (kW) | 52.9 |
| Pulse duration (ms) | 2 |
| Output mode | Linear polarization Gaussian beam |
| Beam waist (mm) | 20.3 |

duration. To reduce RF intensity at the detector, the attenuators were developed to collect the RF beam. The detector output signal and the gyrotron operation were monitored on the data recorder. Cement (1 dB/mm) and paper bundles (0.2 dB/mm) were used as attenuators, for which specifications were obtained from a low-power experiment, as presented in Fig. 5(a).

B. Power distribution measurement for the low-power system

To obtain the characteristics of the corrugated waveguide as an antenna, power distribution measurements with a low-power millimeter-wave transmission system were conducted,

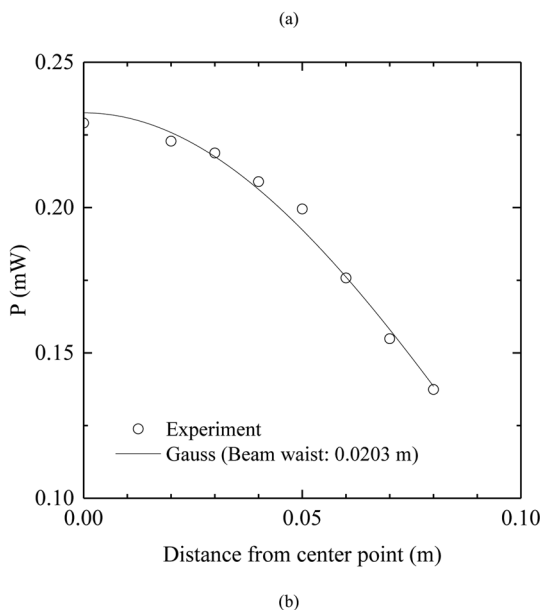
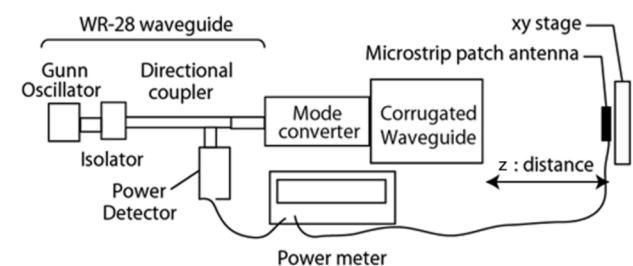


FIG. 5. Power distribution measurement using the low-power transmission system (a). The power distribution was measured at $z = 900$ mm along the x direction (b).

as presented in Fig. 5. The power transmission system consists of the Gunn oscillator, the isolator, the 10 dB directional coupler with the power meter, and a mode converter (General Atomics). The input and received RF power were monitored by using two power sensors (R8466A; Keysight Technologies, Inc.) and a power meter (E4419B; Keysight Technologies, Inc.). The microstrip array antenna, as shown in Fig. 1, was used to measure the RF power because it was difficult to use the rectenna for this low power intensity experiment. Figure 5 portrays power distribution measurements using the low-power millimeter-wave system. The theoretical curve of Gaussian distribution showed good agreement with the experimental RF output.

C. Power distribution measurement for gyrotron beam output

Figure 6 portrays the power distribution measurement by the detector compared with the infrared image normalized

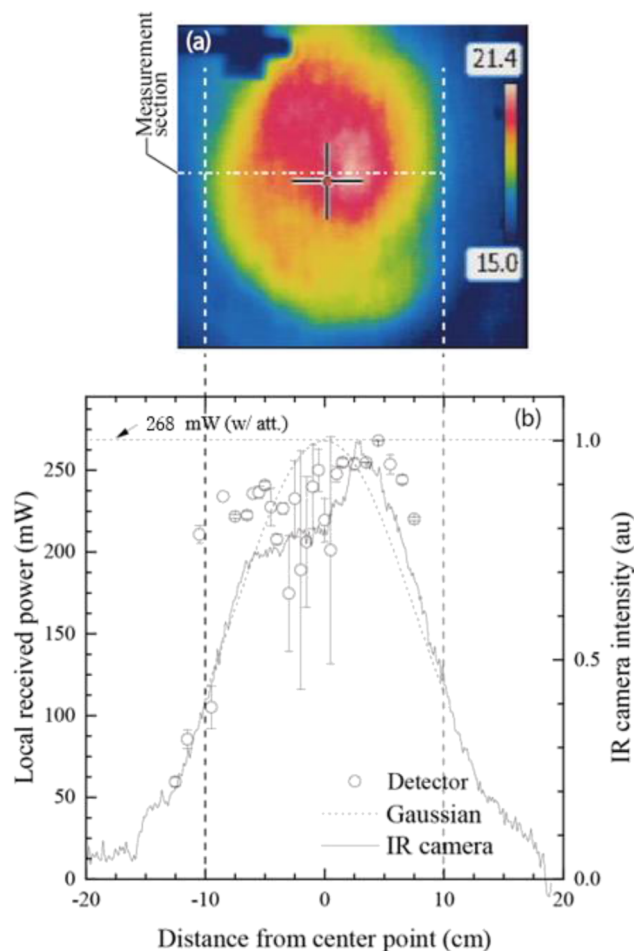


FIG. 6. Infrared imaging on the microwave absorber (a) and RF power distribution with IR camera intensity (b). The distance from the corrugated waveguide aperture is 90 cm. The peak local received power and DC output level were 268 mW and 7.24 mW, respectively.

intensity. Generally, the HE 11 mode of the corrugated waveguide couples 98% to the free propagation with TEM 00 mode of space.²⁵ The experimentally obtained results were compared with the Gaussian distribution curve (theory). An infrared imaging camera (SC7600; FLIR, Inc.) was used to observe the temperature changes on the microwave absorber. As depicted in Fig. 6(a), the temperature on the microwave absorber was increased from 15 °C to 21 °C. The normalized intensity of the infrared camera is depicted in Fig. 6(b). Because the IR images are the accumulated images of the IR camera, the shot-to-shot error is not negligibly small. This point is also found when we compared the IR curve with the single rectenna measurement data. The IR image is almost identical to the Gaussian distribution less than 200 mW power level. The fluctuation effect due to the transmission line error of gyrotron, which will be explained later, significantly appeared near the peak of power distribution.

Furthermore, the detector element position was changed in the measurement section, as depicted in Fig. 6(a). The local received power using the detector is shown as the cumulative data in Fig. 6(b). One datum at the position from -2 cm to 4 cm and the other positions were, respectively, taken during 5 and 3 experimental operations. The maximum received power level and power density of the detector with a 33 dB attenuator were respectively 528.7 W and 97.9 W/cm² near the center point.

Consequently, the local received power in front of the antenna at the center point was 268 mW. The maximum DC output level after the rectifier and the RF input level before the rectifier were respectively 7.24 mW and 25.5 mW. Because the aperture efficiency was 9.5%, the received RF power, 268 mW, decreases to 25.5 mW. At the outside of the beam, the detector measurement results showed good agreement with the infrared camera intensity results. Apart from the peak near the center, the profile of the whole beam is stable. Because the gyrotron output is stable and the RF input power is lower than the breakdown power level of the rectenna, the unknown mechanical vibration of the waveguide transmission line might affect the large standard error near the peak of power distribution. Although it is difficult to find such a small radiation pattern change from the accumulated image, it can be found by a single imaging measurement by the rectenna.

To ascertain the time resolution of the detector, the DC output and RF monitor signal at the miter bend were compared, as portrayed in Fig. 7. The RF signal was obtained via a crystal mount (WDM-346, Nihon Kosuha Co., Ltd.) and a silicon mixer diode (1N53, Advanced Semiconductor, Inc.). The rise time of gyrotron output was 0.4 ms. The pulse duration was 2 ms. As portrayed in Fig. 7, the DC output signal of the rectenna was the common resistor-capacitor curve. The time resolution of the detector is estimated at 0.4 ms from the RC time constant and as 0.8 ms for 90% of the saturation value.

D. Millimeter wave detector operation as a power meter

The total transmission efficiency from attenuated power to DC array rectenna output was evaluated to obtain the

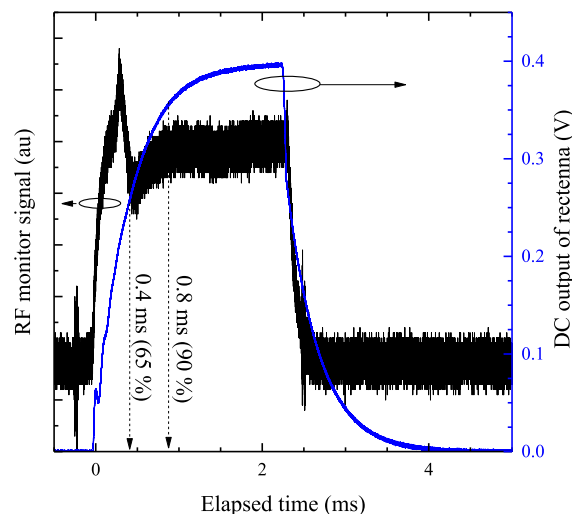


FIG. 7. Time history of the DC output on the rectenna and the RF monitor signal at the miter bend (arbitrary unit).

theoretical DC output power of array rectenna. η_{tot} for the single detector is expressed as

$$\eta_{tot} = \eta_{re}\eta_{apr}\eta_{DC}, \quad (1)$$

where η_{re} , η_{apr} , and η_{DC} respectively denote the effective antenna area efficiency $\eta_{re} = A_{Det}/A_{Beam}$ as shown in Fig. 8, the antenna aperture efficiency, and the RF-DC efficiency for the single detector as provided in Fig. 3. We changed the attenuation value from 20 dB to 40 dB by inserting attenuators. The gyrotron output was fixed at 52.9 kW. From Fig. 8, the beam spot area A_{Beam} was estimated using the Gaussian beam

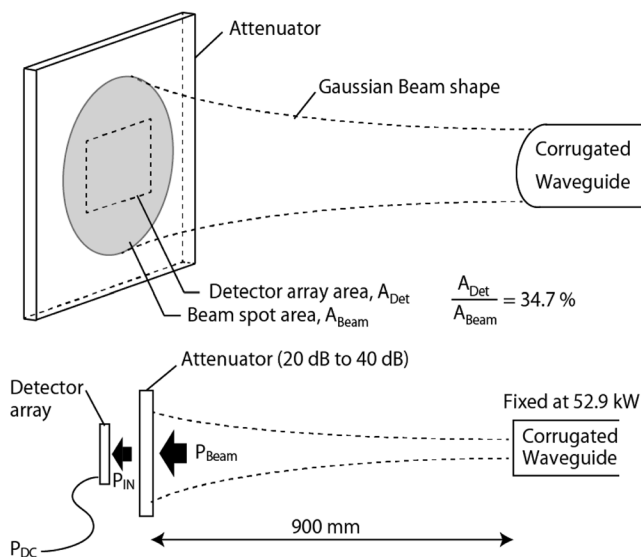


FIG. 8. Effective antenna area: detector array area divided by the beam spot area on the attenuator.

waist a as

$$a = a_0 \sqrt{1 + \left(\frac{\lambda z}{\pi a_0^2}\right)^2}, \quad (2)$$

where z and λ respectively represent the displacement from the irradiation aperture and the millimeter wave wavelength. Also, a_0 is the beam waist at $z = 0$, as obtained from Fig. 5(b). Figure 9 portrays the DC output power of the array antenna and its transmission efficiency as a function of input power without an attenuator. When the input RF power on the detector and the attenuator were, respectively, 9 W and 45 W, the detector was partially damaged because of the excess input power. The theoretical transmission efficiency and the DC output signal were evaluated using Eq. (1), as presented in Fig. 9. Note that the efficiency η_{tot} for a single detector was 0.04%. After the detector was broken, the difference between the theoretical estimation and the experimentally obtained results was increased. Before the diode breakdown, the experimental results were still lower than the theoretical estimation because the variation of the quality of rectenna and attenuator might affect this gap. Besides, the waveguide output was different in the experiment and the theory because theoretical estimation assumed the perfect Gaussian RF beam. Practically, the theoretical gap is not the problem because of the power level calibration. These results reveal that the rectenna array can also serve as a power meter. This proposed power meter can receive high RF input power and can provide a high-speed response. According to the development map for the

RF rectenna, the rectenna detector design can cover at least 300 GHz sub-terahertz gyrotron output.⁸

IV. CONCLUSION

Because it is difficult to achieve both fast response and high power beam measurement for the conventional millimeter wave detector system, such as the IR camera, the water load, and the commercial sensor,¹⁶ this paper proposed the novel and simple detection system for a high power millimeter wave. The detector element consists of the linear polarized microstrip patch antenna with an F-load rectifier, with an RF-DC conversion efficiency of 47.7%. Its output power was 140.8 mW for 295.1 mW input power. The 28 GHz gyrotron output beam distribution was obtained at 900 mm distance from the corrugated waveguide aperture. The results show that the beam intensity at the center was 265 mW. The detector response time was 0.4 ms. Furthermore, the detector demonstration as a power meter showed that the maximum input power was 45 W with 25 detector elements. In the detector experiments, we confirmed the fluctuation of the shot by shot in the center irradiation pattern which was not seen with conventional IR cameras. Therefore, some uncertainties, such as mechanical vibration, are given to the waveguide transmission line. Because our purpose is to use high power microwave from the gyrotron as a wireless power transmission system, the loss-less transmission system design is important. Thus, the results pointed out that the transmission system should be designed which is impervious to influence by external noise, such as a mirror transmission system.

ACKNOWLEDGMENTS

This research was funded by the Japan Society for the Promotion of Science Grant-in-Aid for Scientific Research Grant for Young Researcher No. 16 K 18306.

REFERENCES

1. L. Yujiri, M. Shoucri, and P. Moffa, *IEEE Microw. Mag.* **4**, 39 (2003).
2. H. Park, C. C. Chang, B. H. Deng, C. W. Domier, A. J. H. Donne, K. Kawahata, C. Liang, X. P. Liang, H. J. Lu, N. C. Luhmann, A. Mase, H. Matsuura, E. Mazzucato, A. Miura, K. Mizuno, T. Munsat, Y. Nagayama, M. J. van de Pol, J. Wang, Z. G. Xia, and W. K. Zhang, *Rev. Sci. Instrum.* **74**, 4239 (2003).
3. T. Kariya, R. Minami, T. Imai, M. Ota, Y. Endo, S. Kubo, T. Shimozuma, H. Takahashi, Y. Yoshimura, S. Ito, T. Mutoh, K. Sakamoto, and Y. Mitsunaka, *J. Infrared, Millimeter, Terahertz Waves* **32**, 295 (2011).
4. Y. Hidaka, E. M. Choi, I. Mastovsky, M. A. Shapiro, J. R. Sirigiri, R. J. Temkin, G. F. Edmiston, A. A. Neuber, and Y. Oda, *Phys. Plasmas* **16**, 055702 (2009).
5. J. P. Boeuf, B. Chaudhury, and G. Q. Zhu, *Phys. Rev. Lett.* **104**, 015002 (2010).
6. Y. Oda, T. Shibata, K. Komurasaki, K. Takahashi, A. Kasugai, and K. Sakamoto, *J. Propul. Power* **25**, 118 (2009).
7. K. Shimamura, H. Sawahara, A. Oda, S. Minakawa, S. Mizojiri, S. Suganuma, K. Mori, and K. Komurasaki, *Wirel. Power Transfer* **4**, 146 (2017).
8. S. Mizojiri, K. Shimamura, M. Fukunari, S. Minakawa, S. Yokota, Y. Yamaguchi, Y. Tatematsu, and T. Saito, *IEEE Microw. Wirel. Compon. Lett.* **28**, 834 (2018).
9. M. Thumm, *State-of-the-Art of High Power Gyro-Devices and Free Electron Masers. Update 2016* (KIT Scientific Publishing, Karlsruhe, 2017).

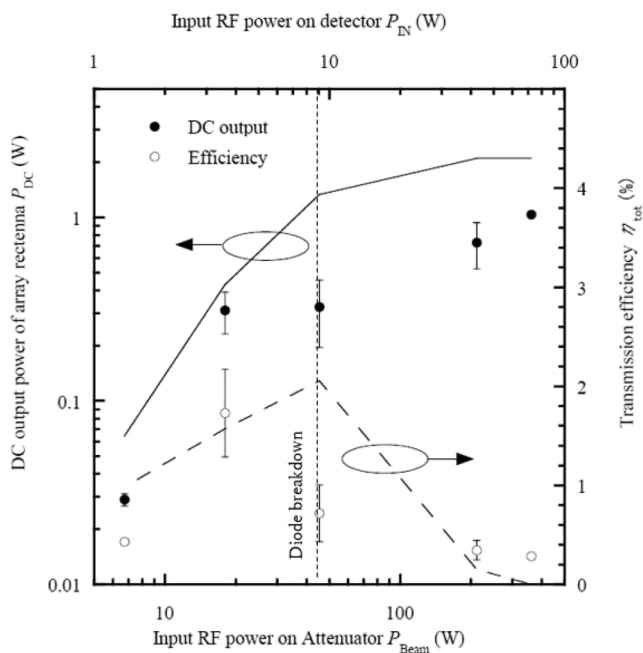


FIG. 9. Array rectenna DC output and its transmission efficiency as a function of input RF power with and without an attenuator. The solid and dashed lines in the figure are the theoretical values. The input RF power on attenuator P_{Beam} was varied by changing attenuation value.

- ¹⁰T. Notake, T. Saito, Y. Tatematsu, A. Fujii, S. Ogasawara, L. Agusu, I. Ogawa, T. Idehara, and V. N. Manuilov, *Phys. Rev. Lett.* **103**, 225002 (2009).
- ¹¹J. W. Ok, S. Choi, B. S. Lee, J. H. Yoon, J. Y. Park, C. S. Shin, M. S. Won, and I. S. Hong, *J. Korean Phys. Soc.* **66**, 349 (2015).
- ¹²S. Jawa, J. P. Hogge, S. Alberti, T. Goodman, B. Piosczyk, and T. Rzesnicki, *IEEE Trans. Plasma Sci.* **37**, 414 (2009).
- ¹³A. V. Chirkov and G. G. Denisov, *Int. J. Infrared Millimeter Waves* **21**, 83 (2000).
- ¹⁴W. Kasperek et al., *Nucl. Fusion* **48**, 054010 (2008).
- ¹⁵M. K. Hornstein, V. S. Bajaj, R. G. Griffin, K. E. Kreischer, I. Matovsky, M. A. Shapiro, and R. J. Temkin, "Design of a 460 GHz second harmonic gyrotron oscillator for use in dynamic nuclear polarization," in *27th International Conference on Infrared and Millimeter Waves* (IEEE, San Diego, CA, USA, 2002), pp. 193–194.
- ¹⁶V. M. Muravev, G. E. Tsydynzhapov, A. A. Dremin, and I. V. Kukushkin, in *2016 41st International Conference on Infrared, Millimeter, and Terahertz Waves (IRMMW-THz)* (IEEE, Copenhagen, 2016), p. 1.
- ¹⁷T. Kariya, Y. Mitsunaka, T. Imai, T. Saito, Y. Tatematsu, K. Sakamoto, R. Minami, O. Watanabe, T. Numakura, and Y. Endo, *Fusion Sci. Technol.* **51**(2T), 397–399 (2007).
- ¹⁸J. Shively et al., "Development program for a 200 kW CW, 28 GHz gyrokystron," Contract No. W-7405-eng-2, Final Report, Varian Associates, Inc., Oak Ridge National Laboratory, April 1976–September 1980.
- ¹⁹H. R. Jory, S. Evans, J. Moran, J. Shively, D. Stone, and G. Thomas, "200 kW pulsed and CW gyrotrons at 28 GHz," in *International Electron Devices Meeting, Washington, D.C., 8–10 December, Technical Digest* (IEEE, 1980), pp. 304–307.
- ²⁰B. Yu, G. Denisov, A. Ereemeev, V. Gorbatushkov, V. Kurkin, G. Kalynova, V. Kholoptsev, A. Luchinin, and I. Plotnikov, *Rev. Sci. Instrum.* **75**(5), 1437–1439 (2004).
- ²¹V. E. Zapevalov, Yu. K. Kalynov, V. K. Lygin, O. V. Malygin, S. A. Malygin, M. A. Moiseev, V. N. Manuilov, E. A. Soluyanov, E. M. Tai, and V. I. Khizhnyak, *Radiophys. Quantum Electron.* **49**, 185 (2006).
- ²²T. W. Yoo and K. Chang, *IEEE Trans. Microwave Theory Tech.* **40**, 1259 (1992).
- ²³N. Shinohara and K. Hatano, *J. Phys.: Conf. Ser.* **557**, 012002 (2014).
- ²⁴S. Ladan, S. Hemour, and K. Wu, in *2013 IEEE International Wireless Symposium IWS 2013* (IEEE, 2013), pp. 7–10.
- ²⁵L. Rebuffi and J. P. Crenn, *Int. J. Infrared Millimeter Waves* **10**, 291 (1989).